Available online at www.sciencedirect.com

SciVerse ScienceDirect

Geochimica et Cosmochimica Acta 109 (2013) 329–344

Geochimica et Cosmochimica Acta

www.elsevier.com/locate/gca

Organic carbon export from the Greenland ice sheet

Maya P. Bhatia [a,*], Sarah B. Das [b], Li Xu [b], Matthew A. Charette [c], Jemma L. Wadham [d], Elizabeth B. Kujawinski [c]

[a] MIT/WHOI Joint Program in Oceanography/Applied Ocean Sciences and Engineering, Department of Geology and Geophysics, Woods Hole Oceanographic Institution, Woods Hole, MA 02543, United States

[b] Department of Geology and Geophysics, Woods Hole Oceanographic Institution, Woods Hole, MA 02543, United States

[c] Department of Marine Chemistry and Geochemistry, Woods Hole Oceanographic Institution, Woods Hole, MA 02543, United States

[d] School of Geographical Sciences, University of Bristol, Bristol BS8 1SS, UK

Received 1 May 2012; accepted in revised form 3 February 2013; available online 14 February 2013

Abstract

Glacial meltwater exports a unique type of organic carbon to marine systems, distinct from non-glacially derived riverine export, potentially capable of stimulating downstream marine primary productivity. Here, we describe for the first time the bulk-level dissolved organic carbon (DOC) and particulate organic carbon (POC) isotopic composition of glacial meltwater draining the Greenland ice sheet (GrIS). These data, in conjunction with an earlier study that investigated the molecular-level composition of GrIS dissolved organic matter, collectively describe the concentration, radiocarbon content, and lability of organic carbon in subglacial discharge from a land-terminating outlet glacier during a melt season. By scaling up our measurements across the ice sheet, we estimate that the annual DOC flux from the GrIS (0.08 Tg/y) is equivalent to that from a small Arctic river (discharge (Q) < 50 km^3/y), and that the annual POC flux from the GrIS (0.9 Tg/y) may be comparable to that of a large Arctic river (Q > 200 km^3/y). The DOC flux is derived primarily from beneath the glacier (subglacial) (>75%) in the early season, and from surface ice-melt (up to 100%) transmitting through the subglacial environment at the peak of the meltseason. The POC flux is primarily derived from the subglacial environment throughout the meltseason. The early season (low flow) glacier discharge contains higher DOC concentrations (0.5–4.1 mg L^{-1}), and exports more enriched carbon ($\Delta^{14}C_{DOC} \sim -250‰$) compared to the peak season (high flow) discharge, when the concentrations are lower (0.1–0.6 mg L^{-1}) and the $\Delta^{14}C$ is more depleted ($\Delta^{14}C_{DOC} \sim -400‰$). Conversely, the POC export (1.4–13.2 mg L^{-1}, $\Delta^{14}C_{POC} \sim -250‰$) shows no temporal variation in either concentration or radiocarbon content throughout the meltseason. Dissolved ion loads in concomitant samples reflected the seasonal evolution of the subglacial drainage system, confirming the influence of subglacial hydrology on the composition of the bulk carbon pools. Based on this work, we conclude that (1) different mechanisms control the DOC and POC flux from glacial systems; (2) chemically-distinct DOC pools are accessed by seasonally-evolving hydrological flow-paths; and (3) the GrIS can deliver labile carbon, which may also be ^{14}C-depleted, to downstream proglacial and marine environments.

* Corresponding author. Current address: Department of Microbiology and Immunology, University of British Columbia, Life Sciences Institute, 2554-2350 Health Sciences Mall, Vancouver, BC, Canada V6T 1Z3.

E-mail address: mayab3@mail.ubc.ca (M.P. Bhatia).

0016-7037/$ - see front matter © 2013 Elsevier Ltd. All rights reserved.
http://dx.doi.org/10.1016/j.gca.2013.02.006

1. INTRODUCTION

Glacial environments possess a dynamic and reactive carbon system (Hood and Scott, 2008; Hood et al., 2009; Pautler et al., 2011). From a glacial–interglacial perspective, *in situ* microbial metabolism of subglacial organic carbon beneath large continental (e.g. the Laurentide) ice sheets could produce CO_2 and CH_4 (Skidmore et al., 2000; Wadham et al., 2008) that may have been released following deglaciation. From a present-day perspective, recent work reveals that modern glacier runoff along the Gulf of Alaska (GOA) is capable of exporting ancient, labile dissolved organic carbon to surrounding coastal ecosystems (Hood et al., 2009). This hypothesis by Hood et al. (2009) has important implications for the coastal waters surrounding Greenland, where the GrIS contributed an estimated $\sim$400 km^3 meltwater runoff in 2010 (Bamber et al., 2012) comparable to the average annual discharge from a large Arctic river (e.g. the Ob River; Dittmar and Kattner, 2003). Despite the fact that GrIS runoff is increasing, particularly to the North Atlantic Ocean (Bamber et al., 2012), there are very few studies of organic carbon export from large ice sheets.

Extant studies have focused primarily on end-member carbon pools found on the ice sheet surface and the bed, rather than on bulk meltwater runoff. These studies reveal that in comparison to riverine, marine, and estuarine environments, organic carbon from the ice sheet surface (i.e. supraglacial snow, ice, and meltwater) and base (basal ice) is nitrogen-rich, containing proteinaceous and other biologically-derived compounds (Bhatia et al., 2010; Dubnick et al., 2010; Pautler et al., 2011). The source of these compounds is presumed to be *in situ* microbial communities on the glacier surface and at the ice-bed interface (Carpenter et al., 2000; Skidmore et al., 2000; Bhatia et al., 2006; Hodson et al., 2008). Other recent studies have suggested that aerosol particles, specifically anthropogenic combustion products (Stubbins et al., 2012), deposited on the glacial surface, are another potential source of organic material to glacial systems (Stibal et al., 2008). A recent review of glacial ice dissolved organic matter (DOM) from 26 glaciers in the European Alps, however, suggests that combustion products are not quantitatively significant in glacially-derived DOM, at least for that region (Singer et al., 2012). Clearly, the origin and nature of the labile component of glacially-derived DOM remains unresolved.

Recent studies have shown that the majority of the meltwater draining the Greenland ice sheet drains first to the bed, and is then discharged via a seasonally-evolving subglacial (beneath the ice) drainage system (Das et al., 2008; Bartholomew et al., 2010; Bhatia et al., 2011). Thus, any study of the contribution of carbon from ice sheets to surrounding coastal oceans needs to be undertaken within the proper context for meltwater outflow (hydrology and volume). Previous work on Alaskan glaciers indicates that glacial runoff possesses a radiocarbon (^{14}C)-depleted signature (Hood et al., 2009). Compositional studies of runoff organic carbon have highlighted the presence of both terrestrial and microbial-derived components (Barker et al., 2006; Bhatia et al., 2010; Dubnick et al., 2010). One potential explanation for these observations is that terrestrial material may be derived from overridden soils and vegetation while the presence of uniquely-adapted subglacial microbes at the glacier bed may provide metabolic by-products (Sharp et al., 1999; Skidmore et al., 2005; Cheng and Foght, 2007). The metabolite pool would retain a ^{14}C-depleted signature if these organisms utilize relict organic carbon sources (Petsch et al., 2001).

Previously, we investigated glacially-derived organic carbon using molecular-level analyses (i.e. ultra-high resolution mass spectrometry; (Bhatia et al., 2010)), providing insight into DOM source and lability. Here, we combine these observations with bulk-level analyses of abundance and radiocarbon content of organic carbon in glacial meltwater to establish a comprehensive description of cycling and export of organic carbon from the Greenland ice sheet. We examine both the dissolved and particulate organic carbon (DOC, POC) pools, since they are likely influenced by different dynamics in the subglacial system, and have different fates in the marine environment. We combine prior results from an isotope mixing model (Bhatia et al., 2011) with the major ion chemistry to gain insight into the evolution of the subglacial drainage system, and the dominant subglacial chemical weathering regimes at our study site. With these results, we test the hypothesis that glacier hydrology plays an important role in dictating the type (concentration, radiocarbon content, source, lability) of organic matter released from glacial systems.

2. FIELD SITE DESCRIPTION

Our study site is located on the southwestern margin of the Greenland ice sheet (Fig. 1), approximately 125-km south of Jakobshavn Isbrae/Disko Bay and 120-km north of Kangerlussuaq. Our field area consists of three land-terminating outlet glaciers (identified here as glaciers 'M', 'N', and 'O') that drain into a large ($\sim$10-km long) proglacial lake (Tycho Brahe So/Qasigiatsigit), which discharges into Arfersiorfik Fjord. The bedrock geology of this area consists primarily of quartz diorite rocks of the Nagssugtqidian Orogenic Complex (K/Ar age 1790–1650 m.y.), most likely from an intrusive sheet metamorphosed in its outer parts (Escher, 1971).

3. SAMPLING OVERVIEW

In this study, sampling was concentrated around 'N' glacier (68°02′34″N, 50°16′08″W), a small ($\sim$5 km^2 catchment) outlet glacier, whose physical characteristics, local meteorology, and hydrology have been described in detail elsewhere (Bhatia et al., 2011). In brief, we proposed that over the course of a meltseason the subglacial drainage at 'N' glacier evolves from a distributed to channelized flow system. We found that the 'Early May' runoff drains a base flow-dominated, hydraulically inefficient network composed of basal water that has been stored for some time at the glacier bed (termed "delayed flow" water in Bhatia et al., 2011) In contrast, the 'Late May' and 'July' runoff drains an increasingly glacial ice melt-dominated, hydraulically efficient network (Bhatia et al., 2011). We identified

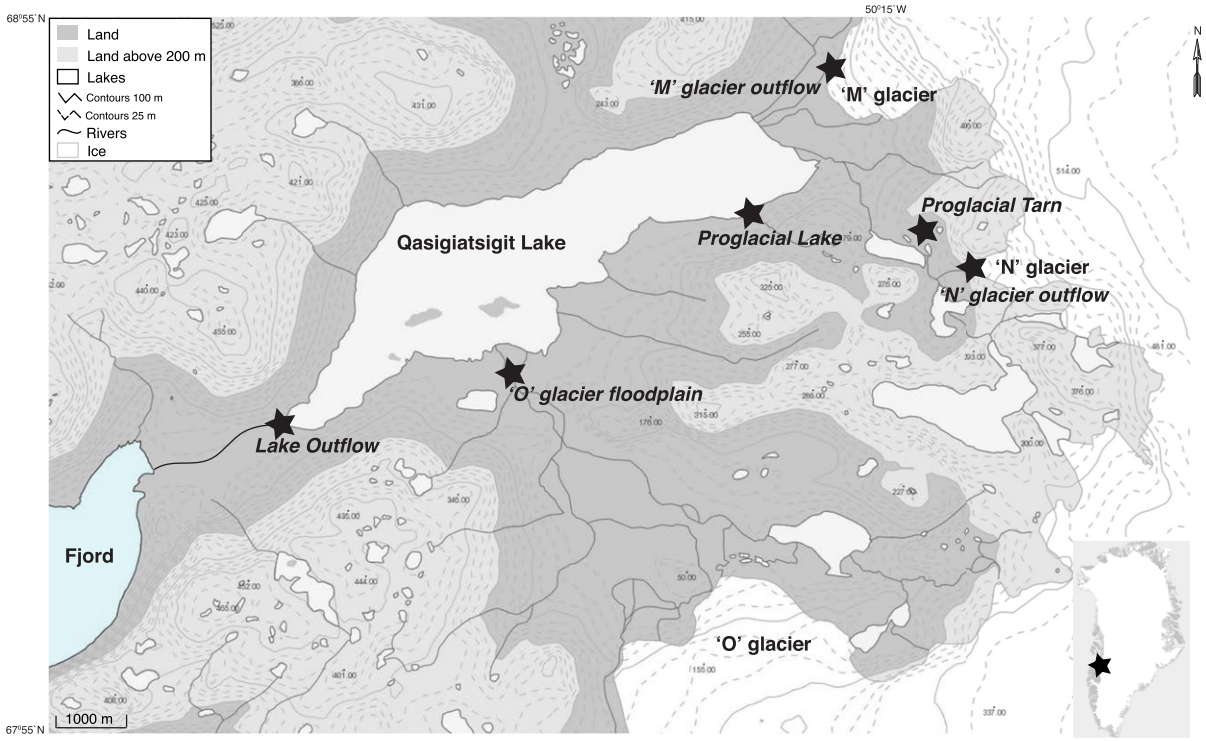

Fig. 1. Map of primary field site on the southwestern margin of the Greenland ice sheet (1:100, adapted from NunaGIS). Approximate sample locations are shown by black stars, and named in the italicized text. Contour elevations are shown in meters.

three time periods with distinct hydrological regimes during the melt season, named 'Early May' (May 18–24), 'Late May' (May 25–June 1), and 'July' (July 10–16). The Early May waters were comprised of $\geqslant$49% contribution from basal waters (waters stored at the ice sheet bed), whereas the Late May and July waters had 12–36% and 5–17% respective contributions from basal waters (Bhatia et al., 2011). Since these time periods have distinct ion and carbon signatures, we retain usage of these terms here. Base flow contributed close to 100% of runoff on May 21st, when we observed our lowest discharge value.

Daily stream samples were collected from the 'N' glacier outflow during the spring (May 16 to June 1) and at the height of the summer melt season (July 10 to July 17) in 2008. Samples were generally collected in the afternoon, local time. Additional proglacial point samples were collected from the 'M' glacier outflow; from the 'O' glacier floodplain; from a small closed basin in front of 'N' glacier (a tarn fed by modern precipitation, abbreviated 'Proglacial Tarn'); from the eastern shore of Qasigiatsigit Lake (abbreviated 'Proglacial Lake'); and from the lake outflow channel (abbreviated 'Lake Outflow'). Additional supraglacial point samples were collected from pooled meltwater on the surface of 'N' glacier (300-m a.s.l., abbreviated 'N' Supraglacial) as well as from an inland site (980-m, abbreviated 'Inland Supraglacial', 980-m) 70-km north-east of our primary field site.

4. METHODS

All glassware was combusted at 450 °C for at least 4 h and all Teflon- and plastic-ware was soaked overnight in 10% hydrochloric (HCl) acid and rinsed extensively with Milli-Q water. Samples were collected in bottles that were rinsed three times with sample (or filtrate, as appropriate) prior to collection. All chemicals were obtained from Thermo Fisher Scientific. Organic solvents were Optima grade or better. Concentrated acids were trace-metal grade or better. Samples for bulk analyses were collected at approximately the same time of day. Samples collected on the same day were generally sampled in the morning and evening.

4.1. Major ion, alkalinity, and nutrient analyses

Water samples for ion and nutrient analyses were collected in 500-mL high-density polyethylene (HDPE) wide-mouth bottles (Nalgene). Samples were filtered immediately through 0.22 μm cellulose acetate membranes (GE) with a polypropylene vacuum filtration apparatus (Nalgene). Filtrate was collected, with minimal headspace, in 20-mL HDPE scintillation vials (Nalgene). Samples were kept as cold as possible in the field, and frozen upon return to the laboratory. Dissolved anions and cations (Cl^-, NO_3^-, NO_2^-, SO_4^{2-}, Na^+, K^+, Mg^{2+}, Ca^{2+}, NH_4^+) were measured by ion chromatography at the Queen's University Facility for Biogeochemical Research on Environmental Change and the Cryosphere (Kingston, ON, Canada). Anions and cations were determined simultaneously on separate systems using a Dionex ICS 3000, following the methods in Lafreniere and Lamoureux (2008). Analytical error for most analyses was less than 10%, based on replicate analyses of samples. The limit of detection (LOD)

was defined as three times the standard deviation of regularly measured low concentration samples. The LODs for the anions were: 0.52 μeq L^{-1} for Cl^-, 0.03 μeq L^{-1} for NO_2^-, 0.12 μeq L^{-1} for SO_4^{2-}, and 0.04 μeq L^{-1} for NO_3^-. For the cations, the LODs were: 0.11 μeq L^{-1} for Na^+, 0.18 μeq L^{-1} for NH_4^+, 0.01 μeq L^{-1} for K^+, 0.11 μeq L^{-1} for Mg^{2+}, and 0.24 μeq L^{-1} for Ca^{2+}. Alkalinity (as HCO_3^-) was calculated from the ionic charge deficit using the ion chromatography data. Following previous studies in glacial catchments (e.g. Wadham et al., 2010b) all cations (excluding NH_4^+) and sulfate concentrations were corrected for their sea-salt derived components using standard ratios to Cl^- reported for these ions in seawater (Holland, 1978). The residual crustal-derived component is denoted with an asterisk (*).

4.2. Dissolved organic carbon (DOC) analyses

Samples for DOC analyses were collected in 250-mL glass bottles. All samples were filtered on-site using a combusted glass filtration apparatus, through a combusted preweighed glass–fiber pre-filter (GF/F; Whatman; nominal pore-size 0.7-μm) and a combusted 0.2-μm Anodisc membrane (Whatman). The GFF pre-filter was kept as cold as possible in the field, and frozen at −20 °C upon return to the laboratory for POC analyses (see below). The 0.2-μm filtrate was acidified to pH 2 with concentrated HCl, and stored in a 40-mL glass vial. Samples were kept as cold as possible in the field and stored at 4 °C upon return to the laboratory. DOC concentrations were quantified as described in Bhatia et al. (2010). The limit of detection (based on instrument blanks) was ~0.02 mg L^{-1}. Analytical error was less than 2% (±0.01 mg L^{-1}) based on replicate injections. Errors on mean values are 1-standard deviation (STD).

4.3. Particulate organic carbon (POC) analyses

POC was determined on the GF/F pre-filter by dynamic flash combustion with thermal conductive detection on a Flash EA1112 Carbon Analyzer (ThermoQuest) at the Woods Hole Oceanographic Institution Nutrient Facility. Samples were fumed with 50% sulfurous acid for 24 h (Verardo et al., 1990), and dried overnight at 50 °C to remove carbonate for POC analysis. An acetanilide certified standard (Microanalysis Limited) was used to make a 9-point standard curve, and blanks and standards were analyzed routinely within each sample run. Analytical error is less than 0.01%, based on replicate standards. The limit of detection for carbon was ⩽0.008 mg L^{-1}. Results are presented as mg L^{-1} and as percent (%) organic carbon. Errors on mean values are 1-STD.

The average discharge-weighted POC and DOC concentrations were calculated using the measured discharge at the time closest to the sample collection. The flux (kg d^{-1}) of POC and DOC from 'N' glacier was calculated as the product of the measured concentrations and the 24-h moving average discharge at the time closest to the collection time (from (Bhatia et al., 2011)). The seasonal DOC and POC fluxes for the entire ice sheet were then calculated by multiplying the average discharge-weighted DOC and POC concentrations by the average ice sheet surface runoff from 1961 to 1990 (251 ± 50 km^3/y) (Bamber et al., 2012).

4.4. Bulk organic radiocarbon and stable carbon isotope analyses

Samples for dissolved and particulate organic radiocarbon ($DO^{14}C$ and $PO^{14}C$, respectively) analyses were collected in 2-L Teflon bottles. One 2-L bottle was used for $DO^{14}C$, and another was used for $PO^{14}C$. The majority of the $DO^{14}C$ samples were filtered on-site immediately after collection, using the DOC protocol described above, except that the 0.2-μm filtrate was stored in 1.25-L Teflon bottles. The filtrate was acidified to pH 2–3 with concentrated phosphoric acid (H_3PO_4), kept as cold as possible in the field, and frozen upon return to the laboratory until analysis. The unfiltered aliquot for $PO^{14}C$ was acidified, and frozen upon return to the laboratory.

For radiocarbon content, $DO^{14}C$ and $PO^{14}C$ samples were thawed at 4 °C, followed by analysis at the National Ocean Sciences Accelerator Mass Spectrometry (NOSAMS) Facility (Woods Hole, MA). DOC was converted into carbon dioxide (CO_2) using an ultraviolet (UV) oxidation and vacuum line system, similar to that described by Beaupre et al. (2007), for ^{14}C analysis on the accelerator mass spectrometer (see Schneider et al., (1994) and Stuiver and Polach (1977) for more details on radiocarbon reporting). Analytical blanks (UV-oxidized acidified Milli-Q water) and reference standards (oxalic acid II (modern ^{14}C) and glycine hydrochloride (^{14}C dead)) were analyzed routinely between samples. The analytical blank was <0.3 μM. The $PO^{14}C$ aliquots were thawed at room temperature, and filtered in the laboratory through a combusted GF/ F pre-filter. The POC on the GFF pre-filter was converted into CO_2 for ^{14}C analysis using high temperature combustion at NOSAMS. For both $DO^{14}C$ and $PO^{14}C$, a split of CO_2 gas was taken for analysis of ^{13}C on a VG Prism-II Stable Isotope Ratio Mass Spectrometer.

4.5. Statistics

All data analysis was conducted in MATLAB, including the linear regressions (Model II, geometric mean) used to estimate the ratios between different anions and cations.

5. RESULTS

5.1. Major ion hydrochemistry

The concentrations of the major dissolved anions (Cl^-, NO_3^-, NO_2^-, SO_4^{2-}) and cations (Na^+, K^+, Mg^{2+}, Ca^{2+}) in the 'N' glacier outflow stream display contrasting trends during the three flow periods distinguished by our isotope-mixing model, with the Early May samples being markedly higher (408–746 μeq L^{-1}), compared to Late May (125–329 μeq L^{-1}) and July (39–79 μeq L^{-1}) (Fig. 2). Over the entire melt season, the sum of crustal cation equivalents (Σ^+_{avg}) had a mean value of 121 μeq L^{-1}. However, the

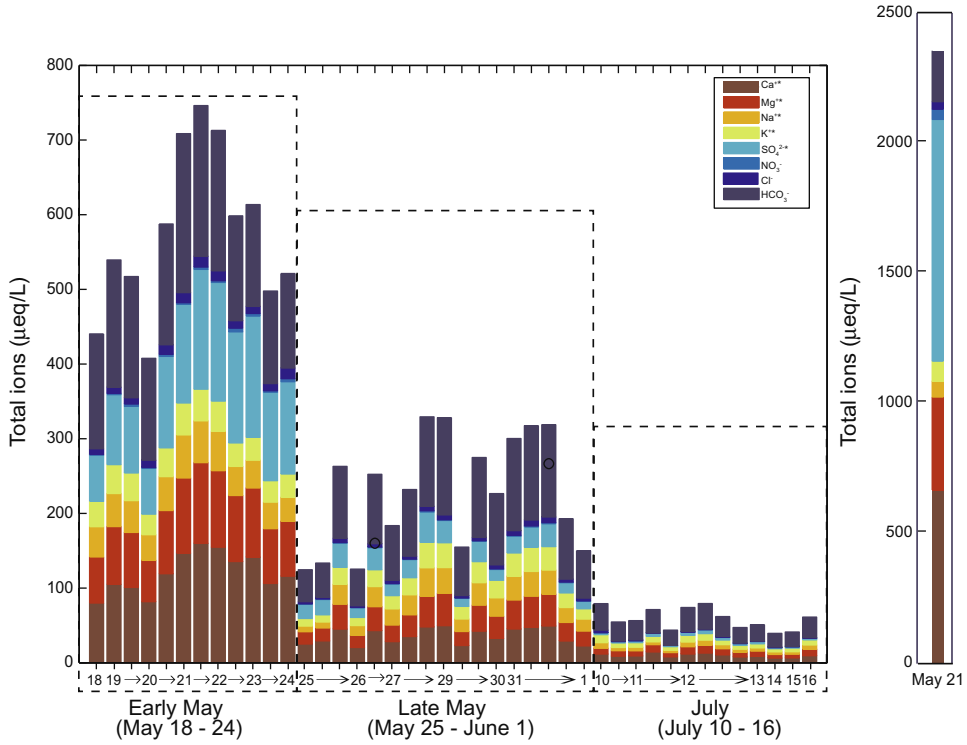

Fig. 2. Total ionic concentrations (in µeq/L) of major dissolved anions and cations in the N glacier outflow waters from May 18 to June 1 and July 10 to July 16, 2008. Time is displayed on the *x*-axis in day of month, and days with multiple samples are indicated with an arrow. The Early May, Late May, and July sample periods are also indicated. The (*) indicates crustal contributions (see text for details). The total ionic concentrations (in µeq/L) in the outlier May 21st base flow sample is shown on the right with its own axes.

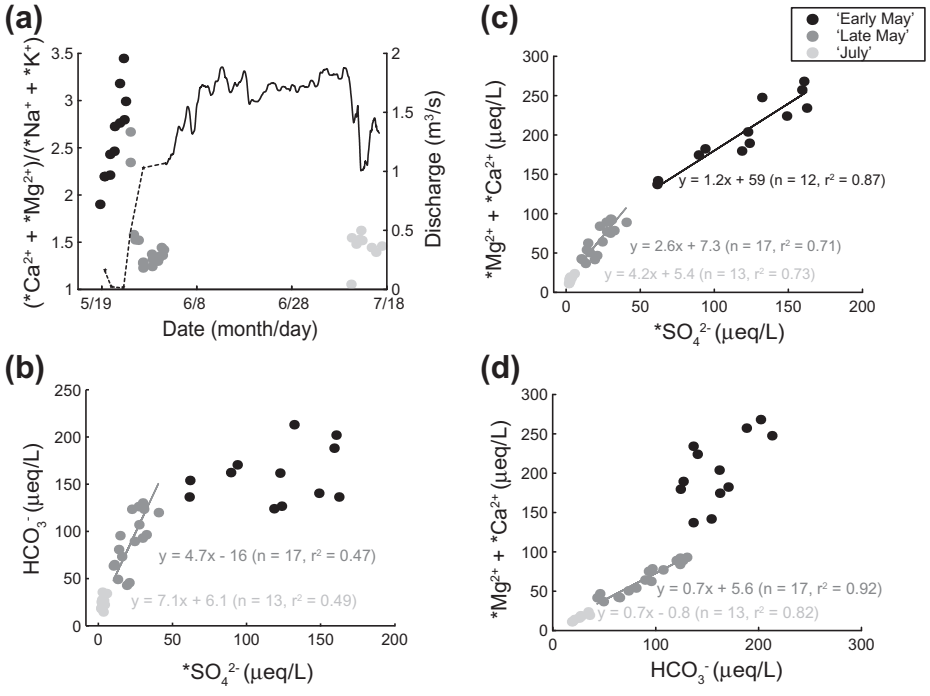

Fig. 3. (a) Ratio of monovalent to divalent crustal cations vs time (for each sampling day), solid line (secondary axis) shows 'N' glacier stream discharge over period of study (dashed line is interpolated). Linear regressions (Model II, geometric mean) separated by time periods (Early May, Late May and July) between (b) HCO_3^- and $^*SO_4^{2-}$, (c) ($^*Mg^{2+} + {}^*Ca^{2+}$) and $^*SO_4^{2-}$ and (d) ($^*Mg^{2+} + {}^*Ca^{2+}$) and HCO_3^- for the 'N' glacier runoff. All regressions presented are significant to the 99% confidence levels.

Early May samples are distinctly more concentrated ($\Sigma^{+}_{avg} = 282$ μeq L^{-1}) compared to Late May ($\Sigma^{+}_{avg} = 112$ μeq L^{-1}) and July ($\Sigma^{+}_{avg} = 29$ μeq L^{-1}). The base flow sample collected on May 21st had an especially high dissolved ion load (2354 μeq L^{-1}), and crustal cation sum ($\Sigma^{+} = 1161$ μeq L^{-1}) (Fig. 2).

We used associations between different ions to gain insight into the nature of the subglacial chemical weathering regime, following Wadham et al. (2010b) The specific ionic indices used were (i) the ratio of monovalent to divalent crustal cations in order to assess the relative contributions of carbonate and silicate dissolution (Fig. 3a), (ii) the association between $^{*}SO_4^{2-}$ and HCO_3^{-} (Fig. 3b) to examine whether microbial oxidation of organic matter is a major influence on meltwater chemistry, and (iii) linear regressions between ($^{*}Mg^{2+} + {}^{*}Ca^{2+}$) and $^{*}SO_4^{2-}$ and between ($^{*}Mg^{2+} + {}^{*}Ca^{2+}$) and HCO_3^{-} (Fig. 3c and d) to estimate the extent to which sulfide oxidation is coupled to carbonate dissolution. Generally, the Early May waters had a higher monovalent to divalent cation ratio compared to the Late May and July waters (Fig. 3a). Only the Late May and July waters showed significant correlation (at the 99% confidence level) between $^{*}SO_4^{2-}$ and HCO_3^{-} (Fig. 3b). All three types of waters had significant relationships between $^{*}SO_4^{2-}$ and ($^{*}Mg^{2+} + {}^{*}Ca^{2+}$) (Fig. 3c); however, only the late May and July waters had significant relationships between HCO_3^{-} and ($^{*}Mg^{2+} + {}^{*}Ca^{2+}$) (Fig. 3d).

5.2. DOC and POC concentrations

The DOC concentrations at 'N' glacier were generally low throughout the melt season (Fig. 4a) with the exception of the May 21 base flow sample (Table 1), which had a DOC concentration of 4.1 mg L^{-1}. Excluding this outlier, on average, the DOC concentrations were slightly higher in Early May (0.61 ± 0.09 mg L^{-1}), compared to Late May (0.39 ± 0.08 mg L^{-1}) and July (0.27 ± 0.15 mg L^{-1}). There was no evident temporal trend in the POC concentrations of the 'N' outflow waters (average concentration $= 3.5 \pm 1.1$ mg L^{-1}, percent organic carbon $= 1.0 \pm 0.5\%$) (Fig. 4b). This average value excludes the May 21 base flow sample (Table 1), which also had a high POC concentration (13.2 mg L^{-1}, percent organic carbon = 9.9%).

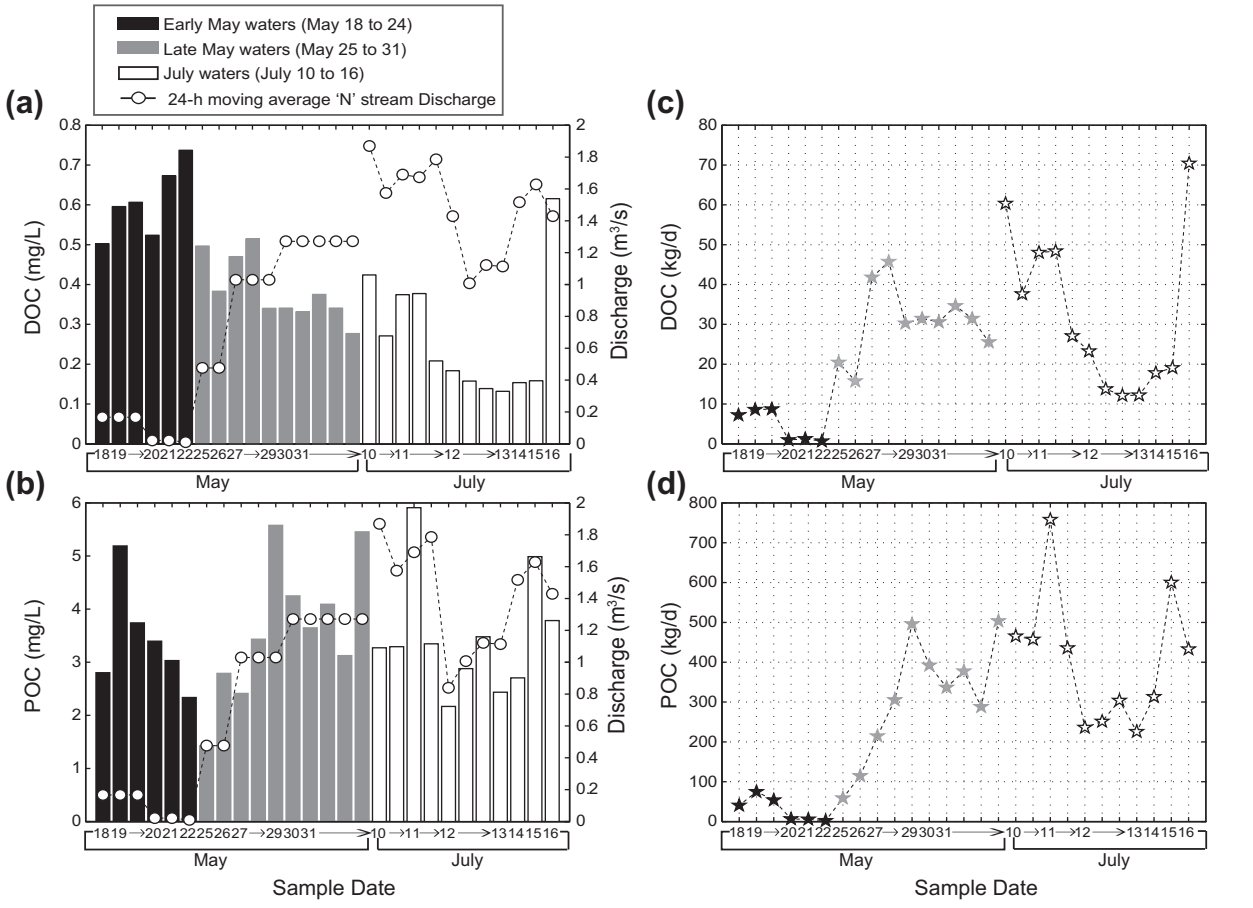

Fig. 4. (a) DOC and (b) POC concentrations in 'N' glacier outflow point samples collected from May 18 to June 1 and July 10 to July 16, 2008, with the discharge measured at the time closest to that of the sample collection time shown on the right *y*-axis. In May the discharge data is limited to point measurements. The daily DOC and POC flux are shown in (c) and (d). Time is displayed on the *x*-axis in day of month, and days with multiple samples are indicated with an arrow. A thin dotted line connects the discharge and flux measurements for ease of viewing, but note that measurements are temporally discontinuous.

Table 1
Mean DOC and POC concentrations (mg L^{-1}) in supraglacial, subglacial, and proglacial samples collected in Early May, Late May, and July. All of the reported measurements represent single samples except for the 'N' glacier outflow (Early May, $n = 7$; Late May, $n = 10$; July, $n = 12$). Errors on mean values are 1-STD.

Sample type	Early May		Late May		July	
	DOC	POC	DOC	POC	DOC	POC
Supraglacial	0.2	0.30	0.2	0.57	–	–
'N' Glacier Outflow	0.6 ± 0.1	3.4 ± 1.0	0.4 ± 0.1	3.6 ± 1.3	0.3 ± 0.2	3.5 ± 1.1
May 21 'N' Glacier base flow outlier	4.1	13.23	–	–	–	–
'M' Glacier Outflow	0.8	2.8	1.2	3.9	0.2	2.2
'O' Glacier Floodplain	1.7	0.76	–	–	–	–
Proglacial Lake	7.4	1.0	0.7	1.7	0.4	–
Lake Outflow	2.7	0.5	–	–	–	–

The DOC concentrations of the point samples collected from the proglacial area in May and July, along with average 'N' and 'M' glacier outflow and 'N' supraglacial samples are shown in Table 1. The 'N' supraglacial samples exhibited the lowest average concentration (0.2 mg L^{-1}, whereas the proglacial samples (i.e. 'O' Glacier Floodplain, Proglacial Lake, and Lake Outflow) were more concentrated (range: 0.7–7.4 mg L^{-1}. The Proglacial Lake sample had a particularly high DOC concentration in early May, although this decreased substantially on June 1 and even further on July 13th. The POC concentrations in the proglacial samples were generally lower than those in the glacier runoff (Table 1).

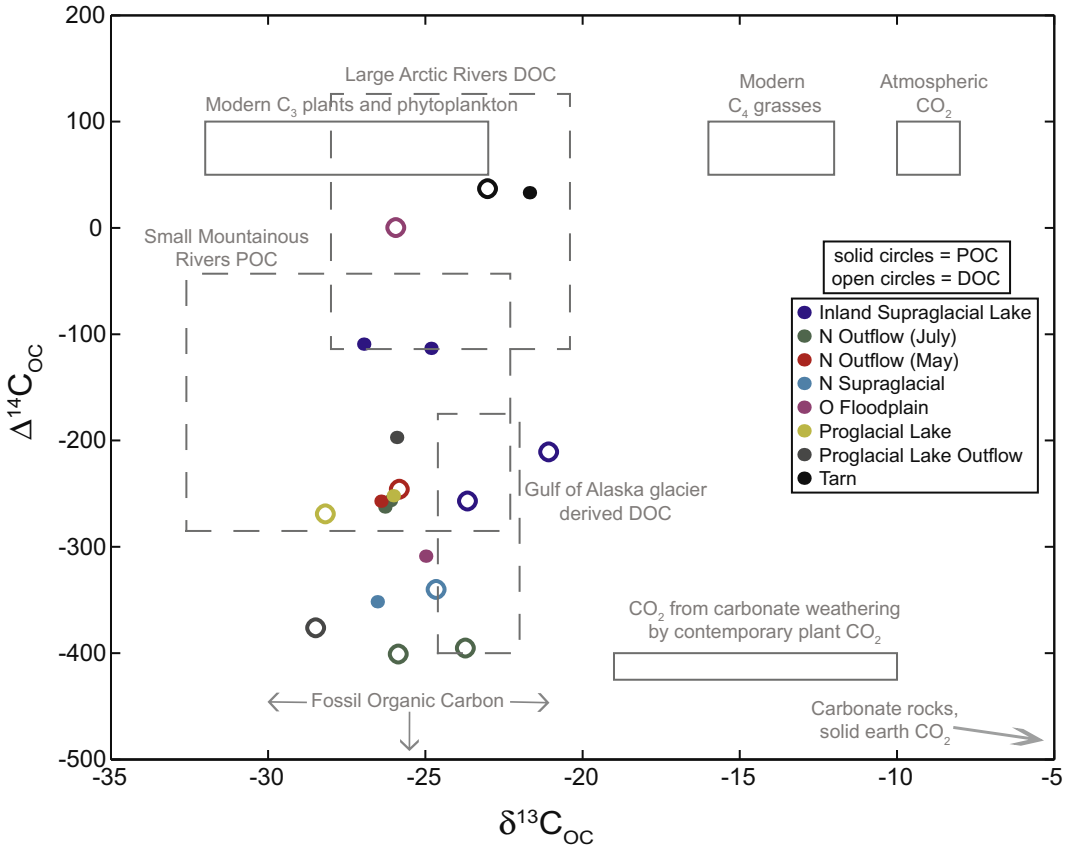

Fig. 5. Dissolved and particulate organic $\Delta^{14}C$ and $\delta^{13}C$ in glacial and proglacial samples collected on the western margin of the Greenland ice sheet. Solid grey boxes illustrate isotopic ranges of end-member carbon sources (Mayorga et al., 2005), whereas dashed grey boxes illustrate literature values for large Arctic rivers DOC (Raymond et al., 2007), small mountainous rivers POC (Raymond and Bauer, 2001a), and Gulf of Alaska (GOA) glacially-derived DOC (Hood et al., 2009). The fossil organic carbon source is radiocarbon dead ($\Delta^{14}C = -1000‰$), and can have $\delta^{13}C$ values ranging from −15‰ to −35‰. (For interpretation of the references to color in this figure legend, the reader is referred to the web version of this article.)

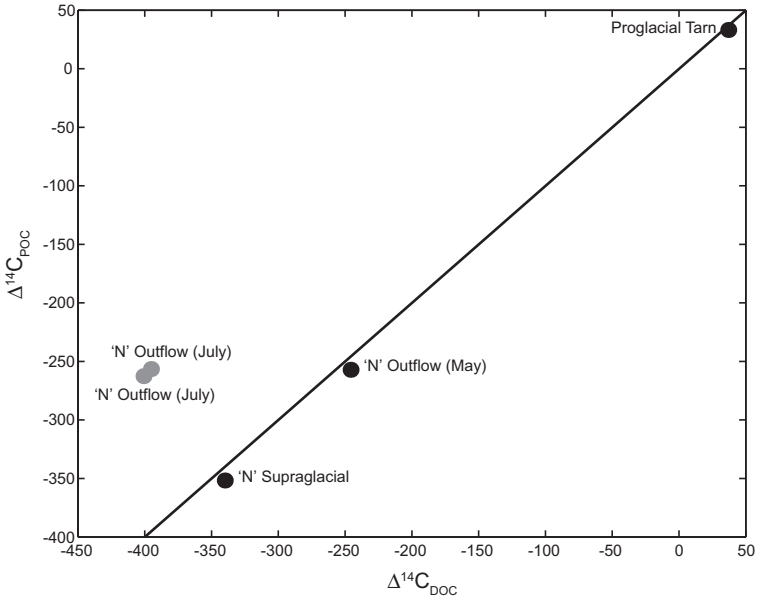

Fig. 6. Dissolved and particulate organic radiocarbon in the 'N' glacier outflow samples collected in May and July 2008, and the samples from 'N' supraglacial water and the proglacial tarn. Samples falling on a 1:1 line (black solid line) are colored in black, whereas samples falling off of this line are shown in grey.

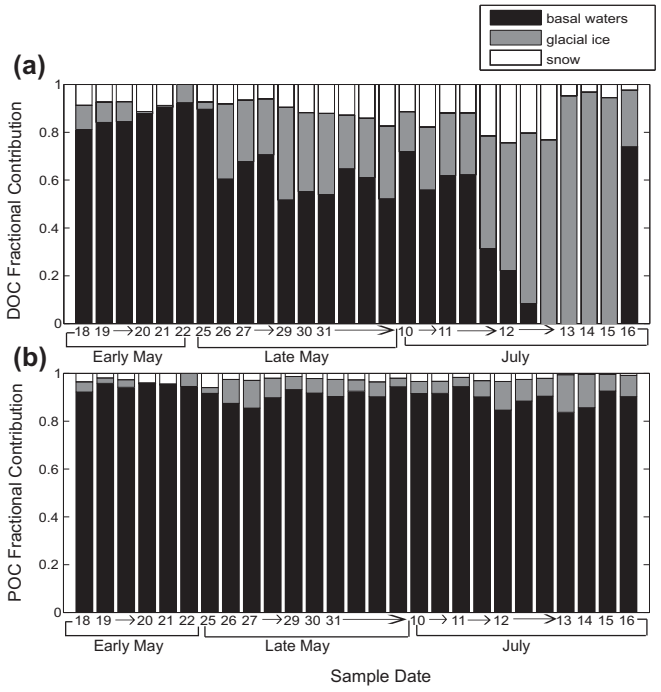

Fig. 7. Estimates of fractional contributions from the basal waters, glacial ice, and snow end-member pools to the total runoff DOC and POC in the 'N' glacier outflow from May 18 to June 1 and July 10 to July 16, 2008. Estimates were calculated using equation 1 (see text for details). Time is displayed on the *x*-axis in day of month, and days with multiple samples are indicated with an arrow. The Early May (May 18 to 24), Late May (May 25 to June 1), and July (July 10 to 16) sample periods are also indicated.

5.3. Bulk organic radiocarbon

The $\delta^{13}C$ and $\Delta^{14}C$ signatures of a subset of supraglacial, subglacial, and proglacial DOC and POC samples are shown in Fig. 5. Generally, an enriched $\Delta^{14}C$ signature represents newly formed (younger) organic carbon, whereas a depleted $\Delta^{14}C$ signature represents relatively older organic carbon. Excluding the proglacial tarn end-member sample, which was enriched in both ^{13}C and ^{14}C, the $\delta^{13}C_{DOC}$ values range from $-21.1‰$ to $-28.5‰$, whereas

the $\delta^{13}C_{POC}$ values only range over ~2‰ (−24.8‰ to −27.0‰) (Fig. 5). The $\Delta^{14}C_{DOC}$ range is ^{14}C-depleted and similar (−211‰ to −401‰) to the $\Delta^{14}C_{POC}$ range (−109‰ to −352‰) with the exception of an enriched $\Delta^{14}C_{DOC}$ sample (0.4‰) from the 'O' glacier floodplain (Fig. 5). Focusing on the subset of samples collected from 'N' glacier and its end-members, we note that the 'N' supraglacial, 'N' subglacial May, and proglacial tarn samples all fall on a 1:1 line between dissolved and particulate radiocarbon (shown in black in Fig. 6), indicating that the dissolved and particle carbon dynamics are coupled for these samples. Conversely, the 'N' subglacial July samples have depleted $\Delta^{14}C_{DOC}$ values relative to their PO $\Delta^{14}C$ values, suggesting de-coupled dynamics (shown in grey on Fig. 6).

In order to determine the DOC contribution and $\Delta^{14}C_{DOC}$ signature of the basal material exported in the 'N' glacier outflow, we employ our previous estimates of the relative proportional snow, ice, and basal flow contributions to the 'N' glacier outflow (Bhatia et al., 2011). Combining this information with the DOC concentrations measured in this study, we can solve for the fractional DOC contribution from the snow, ice, and basal components using:

$$f_c = q_c \times \frac{[DOC]_c}{[DOC]_o} \quad (1)$$

where f_c is the fractional DOC for a component (snow, ice, basal), q_c is the proportional flow contribution of a component (from Bhatia et al., 2011), and [DOC] is the respective DOC concentration in a component ($[DOC]_c$) and in the outflow ($[DOC]_o$). We solved for the ice fraction using an average ice DOC concentration from the surface of 'N' glacier (0.19 ± 0.01 mg L^{-1}) and the average $\Delta^{14}C_{DOC}$ of icemelt from the 'Inland Supraglacial' site (-234 ± 38‰). To calculate the snow fraction, we used the $\Delta^{14}C_{DOC}$ of pooled early-season (frozen) meltwater on the surface of 'N' glacier (−340‰). The resulting fractional DOC contributions are shown in Fig. 7a.

The basal $\Delta^{14}C_{DOC}$ was estimated for the days when we had a bulk radiocarbon value of the 'N' outflow stream (May 19, July 12, and July 16). We defined the mass-balance equation as follows:

$$\Delta^{14}C_{DOC\text{-}o} = f_s \times \Delta^{14}C_{DOC\text{-}s} + f_i \times \Delta^{14}C_{DOC\text{-}i} + f_b \times \Delta^{14}C_{DOC\text{-}b} \quad (2)$$

where the subscripts 'o', 's', 'i', and 'b' refer to the outflow, snow, ice, and basal components respectively. We solved for the $\Delta^{14}C_{DOC\text{-}b}$ term to yield the $\Delta^{14}C$-depleted basal DOC signatures on May 19 (−238‰) and July 16 (−715‰), and a radiocarbon-dead signature (defined as −1000‰) on July 12. Performing an analogous calculation for the POC, we used $[POC]_i = 0.43 \pm 0.19$ mg L^{-1}, $\Delta^{14}C_{POC\text{-}i} = -111 \pm 3$‰, and $\Delta^{14}C_{POC\text{-}s} = -352$‰ to solve for the fractional contributions from the snow, ice, and basal reservoirs to the runoff POC (Fig. 7b). Solving for the basal $\Delta^{14}C_{POC}$ we find depleted basal $\Delta^{14}C_{POC}$ signatures on May 19 (−259‰), July 12 (−289‰), and July 14 (−281‰). The results for both the POC and DOC calculations are not appreciably affected by consideration of the uncertainties in the proportional snow, ice, and basal flow contributions (see sensitivity analysis in Bhatia et al., 2011) and we can conclude that the basal OC is radiocarbon depleted.

6. DISCUSSION

6.1. Subglacial chemical weathering regimes over a meltseason

The major ion hydrochemistry of the 'N' glacier runoff (Fig. 2) is broadly similar in composition to that previously reported from other glacial systems, but is much more dilute ($\Sigma^+_{avg} = 121$ μeq L^{-1}) than typical alpine glacier runoff (Σ^+_{avg} ~700 μeq L^{-1}; Skidmore et al., 2010), suggesting the 'N' glacier has a comparatively unreactive bedrock or shorter subglacial residence times. For comparison to an Arctic surface river, the Σ^+_{avg} of river waters in the non-glaciated Mackenzie River basin is 2900 μeq L^{-1} (Millot et al., 2003). Generally, glacial runoff is a dilute Ca^{2+}–HCO_3^-–SO_4^{2-} dominated mixture, with varying contributions from Na^+ and Cl^- (Σ+ ranging from 10 to 3500 μeq L^{-1}; Tranter, 2003). This composition reflects the fact that subglacial chemical weathering is typically dominated by carbonate (calcite) hydrolysis followed by sulfide oxidation coupled to carbonate dissolution (Tranter, 2003). Previous studies in alpine catchments have shown that even when a bedrock is dominated by silicate minerals, trace carbonates are still preferentially weathered, generating a high ratio of carbonate to silicate dissolution (~5:1 in glacial catchments; Tranter, 2003).

Since Na^+ and K^+ are pre-dominantly derived from silicate dissolution (Wadham et al., 2010b), low ratios of divalent ($^*Ca^{2+} + {}^*Mg^{2+}$) to monovalent ($^*Na^+ + {}^*K^+$) crustal cations (Fig. 3a) indicate enhanced silicate dissolution. The average divalent:monovalent ion ratio in this study was 1.8, a value that is consistent, albeit lower in late May and July, with previous work in other Greenland glacial catchments (Wadham et al., 2010b). The higher divalent:monovalent ion ratio in the Early May runoff (up to 3.5; Fig. 3a) hints that these waters may drain a different chemical weathering environment than later samples. In addition to the high divalent:monovalent ratio found in these waters, we observe an insignificant relationship between HCO_3^- and $Ca^{2+} + Mg^{2+}$ (Fig. 3d), which suggests that carbonate dissolution is not the dominant source for these ions. In contrast, a very strong relationship between $Ca^{2+} + Mg^{2+}$ and SO_4^{2-} (Fig. 3c) suggests that the dissolution of Ca–Mg salts dominates the chemistry of meltwaters in Early May. These chemistries have been observed in subglacial environments where gypsum salts are present in the lithology (Skidmore et al., 2005) and in proglacial environments, where Ca^{2+}–Mg^{2+}–SO_4^{2-} salts are generated by freeze-concentration of moraine and glaciofluvial sediment porewaters over-winter (Cooper, 1988; Wadham et al., 2010a). We are unaware of any gypsum salts within the catchment of 'N' glacier, but freeze-concentration could have occurred in marginal subglacial and proglacial sediments during winter, generating salts which are re-dissolved and entrained in dilute glacial runoff in early May. Field observations show that the sampled runoff in early May drained directly from under the glacier (rather than from ice-marginal sources); thus we assume that any salt re-dissolution occurred subglacially or in proglacial channel-marginal sediments. Stronger relationships in plots of $^*SO_4^{2-}$

vs. HCO_3^- (Fig. 3b) and HCO_3^- vs. ($^*Mg^{2+} + {}^*Ca^{2+}$) (Fig. 3d) in the Late May and July waters indicate that these purported subglacial marginal effects are no longer present.

6.2. Carbon export over a meltseason

The DOC concentrations measured in the 'N' glacier runoff (Fig. 4a) are dilute, but within the range (<1 mg C L^{-1}) previously reported for runoff from other glacial systems (Lafreniere and Sharp, 2004; Barker et al., 2006; Hood et al., 2009). The organic carbon in the 'N' glacier runoff is an amalgamation of supraglacial, englacial, and subglacial sources. Using our model results (Bhatia et al., 2011) in combination with the organic carbon concentrations, we can estimate the mass contributions from the snow, ice, and basal pools to the total runoff DOC and POC (Fig. 7). Since the supraglacial (snow, ice) and englacial environments share ice-melt as their primary carbon source, we can estimate a similar mass contribution from the englacial source as found in the supraglacial samples. Doing this we find that, on average, >75% of the DOC in the early May samples is likely derived from the subglacial environment. This contribution decreases to ~30% in late May, with the remaining ~70% from supraglacial and englacial sources (Fig. 7a). The July DOC runoff (Fig. 4a), on average, could be entirely derived from the supraglacial and englacial sources (Fig. 7a). However, individual July samples with DOC concentrations above 0.2 mg L^{-1} are an exception, and likely have some subglacial contribution (between ~10% and 30%) (Fig. 7a). The May 21st base flow sample (Table 1) is a clear outlier. The carbon mass observed on that day almost certainly has a large subglacial component. From a POC mass balance perspective, since the supraglacial and englacial sources contribute, on average, only ~10% of the mean 'N' glacial runoff POC concentration, we conclude that the majority (~90%) of the runoff POC (Fig. 4b) originates in the subglacial environment throughout the meltseason (Fig. 7b). As with DOC, the POC in the May 21st sample (Table 1) is likely almost entirely subglacial in origin.

The seasonal flux of DOC (Fig. 4c) and POC (Fig. 4d) broadly mimics the discharge curve, illustrating that discharge, rather than concentrations, drives the mass flux of DOC and POC from 'N' glacier. Thus, the majority of glacially-derived organic carbon is annually released in a relatively small period of time (i.e. a few months), during the peak of the summer melt-season. The POC fraction is the quantitatively important pool as it comprises, on average, between 84% and 93% of the total organic carbon mass flux. The proportional average contribution from the DOC pool diminishes from Early May (16%) to Late May (11%) and July (7%), as discharge increases. This is the opposite of major riverine systems (e.g. the Amazon), where DOC is exported in excess of POC (e.g. DOC/POC ~1.8; Hedges et al., 1997). However, since a portion of the POC pool likely settles out quickly upon exit from the glacier terminus, the DOC pool, as the mobile phase, may still have important downstream effects, especially if it is labile.

6.3. Mobilization of subglacial organic carbon pools over a melt season

From a bulk compositional perspective, the DOC and POC of the 'N' glacier outflow samples analyzed in this study were depleted in radiocarbon in both May and July (Fig. 5), suggesting relict carbon sources and/or new microbial production based on depleted in/organic carbon stores. It is important to note that bulk DOC and POC radiocarbon represents heterogeneous mixtures of material, and thus, the ^{14}C signature is likely an amalgamation of enriched and radiocarbon dead material. Few studies exist to provide robust comparison with these data but we can derive some insights from previous work on river systems and glacial runoff into the Gulf of Alaska. The radiocarbon values for DOC exported in the 'N' glacier runoff (Fig. 5) were more depleted than those from large Arctic rivers (Raymond et al., 2007), but within the range of $\Delta^{14}C_{DOC}$ signatures previously reported from runoff draining glaciers along the Gulf of Alaska (Hood et al., 2009). Comparatively, the 'N' glacier runoff $\Delta^{14}C_{POC}$ signatures (Fig. 5) were within the range of previously reported POC from small mountainous rivers (Raymond and Bauer, 2001b). In riverine systems, DOC is derived from recently fixed plant organic matter or is generated during chemical weathering of near surface soil horizons (Raymond and Bauer, 2001b; Benner et al., 2004). Conversely, POC generally enters rivers through mechanical weathering of underlying soil and rock material (Raymond and Bauer, 2001b). Since chemical weathering is a process generally associated with new production, $\Delta^{14}C_{DOC}$ is often enriched relative to concomitant $\Delta^{14}C_{POC}$ in river systems, and typically has a modern or only mildly depleted value (Raymond and Bauer, 2001b). In contrast, POC is often considerably depleted in radiocarbon due to contribution from antiquated carbon sources such as old soil horizons, sedimentary fossil carbon, and sorbed petroleum (Raymond and Bauer, 2001b). Our 'N' glacier runoff data contrast with river systems in that the $\Delta^{14}C_{DOC}$ is more depleted than the $\Delta^{14}C_{POC}$ and becomes increasingly so over the meltseason (Fig. 6). Thus we must invoke a different mechanism to explain the glacial runoff $\Delta^{14}C_{DOC}$ values.

We hypothesize that the different $\Delta^{14}C_{DOC}$ signatures in the May and July runoff are a function of seasonally-evolving subglacial hydrological conditions, whereas the constant $\Delta^{14}C_{POC}$ signature is that of the bulk material overridden by the ice mass. For the DOC pool, this hypothesis is consistent with our previous work at 'N' glacier speculating that the seasonal head-ward evolution of the subglacial drainage system resulted in supraglacial meltwaters accessing relict subglacial organic carbon stores in July during swift passage through the subglacial environment (Bhatia et al., 2010). A mass-balance calculation of the July basal $\Delta^{14}C_{DOC}$ (see Section 4.3) further supports this hypothesis, revealing that the late-season waters are accessing antiquated, radiocarbon-dead basal material. Since the July runoff waters are characterized by very low DOC concentrations, even a small mass contribution of $\Delta^{14}C$-dead material would yield a more depleted bulk $\Delta^{14}C_{DOC}$ signature. Conversely, in May, when the subglacial drainage sys-

tem contains a large base flow component, and is potentially draining saturated porewaters near the ice margin, the basal $\Delta^{14}C_{DOC}$ is similar to that of the outflow signature (Section 4.3). Thus, the DOC pool is sensitive to shifts between the distributed and channelized drainage systems because its contents are mobile, and its concentrations are very low.

We also consider an alternate hypothesis, namely that radiocarbon-dead surface-derived hydrocarbons (or anthropogenic aerosols) may explain the depleted glacial runoff $\Delta^{14}C_{DOC}$ signatures (Stubbins et al., 2012). On a quantitative basis, nearly all of the DOC export in July can be supplied from supraglacial sources and the depleted July values are consistent with some contribution of radiocarbon-dead material. However, the values of July runoff are depleted relative to the $\Delta^{14}C_{DOC}$ measured in inland supraglacial lakes, our most representative samples of the supraglacial meltwater draining to the bed in July. Specifically, the $\Delta^{14}C_{DOC}$ signature of the supraglacial samples (mean = −234‰) is enriched compared to the July runoff $\Delta^{14}C_{DOC}$ signature (mean ∼ −400‰). The approximately 150‰ difference between these two signatures hint at another more ^{14}C-depleted, potentially subglacial, carbon source accessed by the supraglacial meltwaters during transit through the subglacial environment. Compound-specific (or class-specific) radiocarbon analysis is needed to answer these questions definitively.

The majority of the 'N' runoff $\Delta^{14}C_{POC}$ signatures are within the range of previously reported $\Delta^{14}C_{POC}$ from small mountainous rivers (Fig. 5). Thus, we propose that, akin to small mountainous rivers, a relict soil/rock contribution from the subglacial environment yields the depleted glacial runoff $\Delta^{14}C_{POC}$ signature (Raymond and Bauer, 2001b). A mass balance calculation of the basal $\Delta^{14}C_{POC}$ pool confirms that the bulk runoff $\Delta^{14}C_{POC}$ signature is primarily driven by the subglacial contribution (Section 4.3). In comparison to the DOC pool, the runoff POC pool is much larger (in mass), and thus is less susceptible to variable mass contributions resulting from changes in the subglacial drainage system. As a result, its radiocarbon content is invariant with hydrology (Fig. 6) and the POC in general is likely affected more by regional-scale ice sheet behavior than by seasonal hydrology.

The ice margin across our study region has varied considerably over the past tens of thousands of years, which has important implications for the interpretation of our radiocarbon values. Generally, the GrIS has expanded during cooler periods in Earth's history, and retreated during warmer periods (Alley et al., 2010). The ice sheet was at a maximum extent (offshore onto the continental shelf) at the last glacial maximum (∼24 ka) and then retreated slowly (∼1 km/100 y) until the beginning of the Holocene (∼10 ka) (Alley et al., 2010). The rate of retreat then increased (∼3 km/100 y) with the ice sheet reaching a position near or inland of its present margin by ∼7–6 ka (Brink and Weidick, 1974). Evidence from around Disko Bay (north of our study site) shows this extensive early- to mid-Holocene retreat was then followed by numerous subsequent periods of advance and retreat through the present day. Most notably, there were three major periods of regional re-advance within 5–10 km of the present ice margin position at ∼4800–4000 y BP, ∼2500–2000 y BP, and 800–700 y BP (Brink and Weidick, 1974; Weidick and Bennike, 2007). Following this, the ice sheet margin underwent several more minor retreats and re-advances, culminating in ice sheet retreat ongoing since the end of the Little Ice Age. Based on this regional history of multiple retreat and advance cycles throughout the Holocene, it is reasonable to draw the conclusion that the GrIS margin at our field site may have been inland of its present location within the past few thousand years, and thus the outlet glaciers may be overriding organic carbon fixed during that time period.

The 'N' runoff $\Delta^{14}C_{POC}$ values equate to ∼2320–2390 y BP (Fig. 6). These ages are consistent with a Holocene re-advance in the Disko Bay region ∼2500–2000 y BP (Brink and Weidick, 1974; Weidick and Bennike, 2007). At this time, soil and vegetation which had developed since the last glacial retreat in the forefront of the ice margin would be overridden, thus providing an explanation for our observed $PO^{14}C$ values. Any organic material from the last interglacial period (∼130,000 y BP) would be radiocarbon dead (⩾∼50,000 y BP), and thus our observed younger $PO^{14}C$ values indicate that the organic matter is from a Holocene advance. However, we should re-iterate that bulk $PO^{14}C$ is likely a reflection of the amalgamation of material with different ages, and compound-specific radiocarbon analyses would be required to tease apart the ages of the different components.

6.4. Organic carbon source and lability

The bulk-level $\Delta^{14}C$ differences between the May and July 'N' outflow samples are consistent with our previous work at 'N' glacier showing that the DOC composition exported in late May and July differs on a molecular level (Bhatia et al., 2010). Using ultra-high resolution mass spectrometry we showed that the July outflow had a higher proportion of lignin and terrestrial-like material, consistent with the flushing of relict organic carbon from overridden soil and vegetation during the high-discharge meltseason. Comparatively, the organic carbon in the May outflow, though still possessing terrestrial-like compounds, had distinct protein-like and lipid-like signatures. We previously ascribed these signatures to microbial metabolic influences on DOC composition (Bhatia et al., 2010), but these influences may be insufficient to be detected at the bulk level. The bulk $\delta^{13}C$ signature is commonly used by biogeochemists (e.g. Hedges et al., 1997) to glean source information. Using these data, we find that 'N' glacier runoff sampled on May 19, July 12, and July 14 had similar $\delta^{13}C_{DOC}$ signatures (Fig. 5) which all fell within the range of a terrestrial (C3 plant) derivation (Hedges et al., 1997). This indicates that the differences observed at the molecular level (Bhatia et al., 2010) are not large enough to be reflected in the bulk $\delta^{13}C$ signature.

However, a general consideration in the combination of bulk- and molecular-level analyses is that each of these approaches has intrinsic advantages and disadvantages. Bulk measurements such as stable isotopic compositions and radiocarbon content provide information on the major

components comprising the organic carbon pool. But they are limited because they can be insensitive to subsidiary constituents, and can only differentiate broad source perspectives (Hedges et al., 1997). Conversely, although molecular-level analyses are highly sensitive to specific components of the organic carbon pool, they necessarily offer perspective on only select constituents or can be biased by trace component contributions. Given these caveats, our previous work using ultra-high resolution mass spectrometry still yields some insight into the lability of glacially-derived organic matter, showing that (i) protein-like and lipid-like compounds are present in both the May and July 'N' glacier outflow samples, and (ii) that nitrogen-containing molecules may be major contributors to glacial DOM, compared to riverine and open ocean DOM (Kujawinski et al., 2009; Bhatia et al., 2010).

6.5. Evidence for microbially-mediated subglacial chemical weathering?

One potential hypothesis for the origin of the nitrogen-rich DOM in glacial systems is that it is derived from proteinaceous material associated with subglacial microbial communities (Lafreniere and Sharp, 2004; Barker et al., 2006; Hood and Scott, 2008). To investigate this hypothesis in our system, we examined the bulk runoff hydrochemistry for evidence of microbial activity facilitating subglacial chemical weathering beneath 'N' glacier. Previous studies in glacial environments have shown that a subglacial runoff signature significantly perturbed from that expected from a purely abiotic system can be indicative of active microbial communities (Tranter et al., 2002). We acknowledge that it can be difficult to ascertain subglacial biogeochemical processes solely from bulk runoff waters, particularly those without a large subglacial (basal) component (Tranter, 2003). Consequently, we focus our analysis on the Late May waters which are characterized by a high basal meltwater fraction and lack the likely influence of Ca^{2+}–Mg^{2+}–SO_4^{2-} salts dissolution. Two reactions which have been previously documented to be microbially-mediated in subglacial environments are (i) oxidation of organic matter, and (ii) sulfide oxidation (Wadham et al., 2010b).

Carbonate hydrolysis is generally the first reaction to occur when dilute supraglacial meltwater interacts with the glacier bed, and results in the rapid generation of HCO_3^- and $^*Ca^{2+}$ independently of sulfate (Wadham et al., 2010b). This gives rise to a y-intercept of ~220 μeq L^{-1} in plots of $^*SO_4^{2-}$ vs HCO_3^- (Wadham et al., 2010b), which reflects the theoretical solubility of calcite in pure water at 0 °C (Tranter et al., 2002). A y-intercept above 220 μeq L^{-1} suggests an additional source of CO_2 to the subglacial meltwaters, most likely from microbial oxidation of organic matter, which subsequently provides protons for dissolution processes (Wadham et al., 2010b). The Late May samples exhibit significant linear relationships between $^*SO_4^{2-}$ and HCO_3^- and both have y-intercepts well below 220 μeq L^{-1} (Fig. 3b). These low y-intercepts may indicate that little (or no) microbial-generated CO_2 provides protons for carbonate dissolution in bulk runoff during these time periods. There are a number of explanations for this phenomenon including: (a) the silicate bedrock beneath 'N' glacier is not favorable to large-scale microbial colonization; (b) microbial CO_2 is generated in subglacial sediments, where it fuels dissolution processes, but sediment porewaters are fully or partially hydrologically decoupled from the major active drainage pathways from late May onwards (Wadham et al., 2010b). The former explanation is based on previous work suggesting that hard bed-rock systems such as silicates are less amenable to microbial colonization than systems with softer bedrocks such as carbonates (Wadham et al., 2010b). However, the higher DOC concentrations in the early season, particularly in the base flow on May 21st (Table 1), hint that an available organic carbon source for microbial oxidation is present in the 'N' subglacial environment at certain time periods, potentially supporting explanation (b).

High sulfate concentrations in subglacial meltwaters have previously been found to be a consequence of microbially-mediated anoxic sulfide oxidation (Tranter et al., 2002). Sulfide oxidation consumes oxygen, and microbial mediation hastens this process, thus driving regions of the subglacial system anoxic (Sharp et al., 1999). The maximum sulfate concentration that can be generated from sulfide oxidation using oxygen-saturated waters at 0 °C is ~400 μeq L^{-1} (Tranter et al., 2002). Thus, runoff SO_4^{2-} concentrations well above this value suggest alternative oxidizing agents (e.g. Fe^{3+}) are present at the glacier bed, and additional sulfate contributions may be generated via microbially-mediated anoxic sulfide oxidation (Tranter et al., 2002). The Late May 'N' glacier outflow waters exhibit sulfate concentrations (10–41 μeq L^{-1}) well below 400 μeq L^{-1} (Fig. 2), thereby providing no immediate evidence for microbially-mediated anoxic sulfide oxidation. We should note however, that at Haut Glacier d'Arolla, a similarly-sized Swiss Alps glacier with a schist-gneiss-amphibolite bedrock, sulfate concentrations in the bulk runoff are typically less than 200 μeq L^{-1}, but borehole waters sampled at the bed can have a sulfate concentrations up to 1200 μeq L^{-1} (Tranter et al., 2002). Thus, a similar situation may be present at our study site in that the bulk runoff waters are substantially diluted by a glacial ice component, and thus bulk runoff concentrations do not truly represent local sulfate concentrations in subglacial sediments. The May 21st sample of 'N' glacier runoff, which drained the lowest measured discharge waters with the largest modeled base flow component (Bhatia et al., 2011), displayed the largest sulfate concentration at 929 μeq L^{-1}, well above 400 μeq L^{-1}. It is unclear, however, whether this composition reflects meltwater drainage from basal regions that support microbially-mediated anoxic sulfide oxidation.

We conclude from these data that the effect of microbial activity at the ice sheet bed is not sufficient to significantly affect the bulk signature of the major ion chemistry in a similar fashion to that previously observed in some glacial systems where base flow dominates bulk runoff. This may also reflect poor hydrological connectivity between microbially active areas (e.g. sediments) and major conduits at the ice sheet bed. The hydrochemistry and DOC concentrations observed in the base flow (May 21st) sample is compelling evidence that microbial activity is able to influence

subglacial DOM character in specific micro-environments (e.g. water-saturated sediment porewaters), which only affect the bulk runoff signature in the early (low discharge) season. This supposition is further supported by our molecular-level composition analysis of runoff DOM, which revealed a discernable microbial signature in the May runoff that was swamped by an overwhelming terrestrial signature in July runoff (Bhatia et al., 2010).

6.6. Decoupling of radiocarbon and lability in glacial systems?

When examining the relationship between radiocarbon and lability in glacial systems, it is essential to note that the bulk radiocarbon and molecular-level compositional FT-ICR MS data represent different qualitative and quantitative fractions of the DOM pool. Although it represents the larger fraction of the sample, the bulk data may hide important, albeit subtle, differences at the molecular level. Given this unavoidable disconnect, two possibilities can explain the observed combination of proteinaceous molecular composition and ^{14}C-depleted DOC in the 'N' glacial runoff: (1) the labile material is modern, but other radiocarbon-dead material is also present, or (2) the labile material is radiocarbon dead.

In the first possibility, although the bulk $^{14}C_{DOC}$ signature is depleted, the labile component of the DOM pool is not necessarily ^{14}C-depleted, and in fact may be ^{14}C-enriched, representing new production from modern carbon sources. One potential source of modern carbon would be photosynthetic production on the glacial surface (e.g. Hodson et al., 2008). Microbial communities have recently been documented on the Greenland ice sheet surface (Hodson et al., 2010; Stibal et al., 2012), and labile carbon derived from their autotrophic activities (Pautler et al., 2012) could be in-washed to the bed via meltwaters draining to the base at the peak of summer. At the bed, this carbon could further support subglacial heterotrophy in the subglacial sediments (Tung et al., 2006) and basal ice (Yde et al., 2010) at the GrIS margin. Heterotrophic metabolism and its by-products could also contribute to the observed labile component of the DOM pool. Simultaneously, other radiocarbon-dead material (e.g. soot particles) could also be present on the glacier surface (Bhatia et al., 2010; Stubbins et al., 2012), or at the glacier base (e.g. previously overridden organic matter) (Barker et al., 2006), yielding the overall bulk ^{14}C-depleted signature in the runoff. As noted above, a small-mass contribution of ^{14}C-depleted material would have a disproportionately large impact on bulk radiocarbon, driving it to increasingly depleted values.

Alternatively, in the second possibility, if the labile material in glacial ecosystems is indeed radiocarbon dead, we can envision two potential mechanisms capable of creating this material: one involving active microbial communities, and the other not. In the latter case, both the depleted $\Delta^{14}C_{DOC}$ values typical of glacial systems (Hood et al., 2009), and the observed compositional characteristics (protein-like molecular signature (Bhatia et al., 2010)) can be explained by the retention of labile DOM fractions in the soils and vegetation initially overrun during past periods of glacial advance. Thus, although the organic matter may be depleted in radiocarbon, owing to its ultimate derivation from previously overridden soils and vegetation, it may still possess some labile components since the ice cover could inhibit the full range of metabolic reactions present in oxygenated soil environments. In effect, the glacier or ice sheet acts as a freezer, preserving the labile components of the organic matter, which are then exported in the runoff.

However, recent studies have revealed that microbial communities are present in both the supraglacial (Stibal et al., 2012) and subglacial (Tung et al., 2006; Yde et al., 2010) GrIS environments. Thus, the proteinaceous, ^{14}C-depleted material may be the result of subglacial microbial communities utilizing relict organic carbon at the glacier base, resulting in the ^{14}C-depleted signature (Petsch et al., 2001). It is likely that some degree of microbial community is present at our site, but the rate(s) of its metabolic activities may not be sufficient to affect the bulk hydrochemistry signature. Nonetheless, its influence appears to still be present at a molecular-level in the DOM composition.

In most aquatic systems, radiocarbon signature and lability are coupled concepts, since material depleted in radiocarbon is considered to be old, or relict, organic carbon whose labile components have long-since been consumed (Raymond and Bauer, 2001a). However, in glacial systems, we propose that these concepts may be decoupled, either because of (a) new microbial production from relict organic carbon sources or (b) the preservation of labile components in material overridden by the ice sheet long ago. The relative importance of (a) and (b) cannot be constrained without compound-specific radiocarbon analyses. These measurements require very large sample volumes and as such are not logistically possible at this time. As a result, the link between molecular-level composition and age of dissolved organic matter remains unknown.

7. IMPLICATIONS AND CONCLUSIONS

Glacial runoff draining the Greenland ice sheet may export a unique brand of organic carbon, distinct from riverine organic carbon. Both riverine and glacial dissolved organic carbon has a terrestrial δ^{13}C signature and is nitrogen rich (Bhatia et al., 2010). However, relative to riverine organic carbon, glacial organic carbon has lower DOC concentrations, higher POC concentrations, and is depleted in $\Delta^{14}C_{DOC}$ (Hedges et al., 1997). Given future climatic warming scenarios, glacial runoff and associated fluxes of glacially-derived DOC and POC to the marine environment may become increasingly significant (Hood et al., 2009; Bamber et al., 2012). In order to estimate the current magnitude of these fluxes, we cautiously use our results from 'N' glacier to calculate an annual carbon export for the entire GrIS.

Mean surface runoff from the Greenland ice sheet from 1961 to 1990 was 251 ± 50 km^3/y (Bamber et al., 2012) which is comparable to the annual discharge from the Mackenzie river (249–333 km^3/y) (Bamber et al., 2012). Using this discharge estimate and the average discharge-weighted DOC (0.32 mg L^{-1}) and POC (3.7 mg L^{-1}) concentrations measured at 'N' glacier, we estimate an annual export of

0.08 ± 0.02 Tg of DOC and 0.9 ± 0.2 Tg of POC from the Greenland ice sheet. This DOC flux is comparable to a recent estimate from the Gulf of Alaska glaciers (0.13 Tg/y) and within the range of smaller Arctic rivers (e.g. Yana: 0.09 Tg/y) (Dittmar and Kattner, 2003). Conversely, our estimated Greenland ice sheet POC flux is of a similar order of magnitude to that from the Mackenzie (1.8–2.1 Tg/y), the principal river POC contributor to the Arctic ocean (Dittmar and Kattner, 2003).

Glacial runoff may also contribute a pre-aged end-member to the oceanic DOC and POC pools. Similar to Arctic river systems, the majority of the annual organic carbon exported by glacial systems occurs during a short time period, when discharge is at its peak. However, in contrast to river systems (Benner et al., 2004), the base flow exports comparatively more ^{14}C-enriched DOC, whereas the peak flow exports more ^{14}C-depleted DOC, compared to surface (between −150‰ and −400‰) and deep (down to −540‰ in North Pacific Deep Water) ocean waters (McNichol and Aluwihare, 2007). Both the base and peak flow export a ^{14}C depleted POC pool (−257‰ to −263‰) compared to the surface ocean $\Delta^{14}C_{POC}$ signature, which is generally enriched in ^{14}C (Druffel and Bauer, 2000; McNichol and Aluwihare, 2007), and the deep ocean $\Delta^{14}C_{POC}$ (e.g. −111‰ in the Southern Ocean) (Druffel and Bauer, 2000). On a global scale, any glacial contribution is likely orders of magnitude too small in comparison to the standing surface organic carbon inventory to influence the oceanic $\Delta^{14}C_{DOC}$ or $\Delta^{14}C_{POC}$ signatures. However, export of glacially-derived organic carbon from Greenland outlet glaciers may still have localized biogeochemical impact in the coastal North Atlantic and Arctic Oceans. These fluxes will only increase as surface melt on the ice sheet surface increases. Furthermore, the DOC flux may disproportionally increase as the subglacial drainage system extends and develops further inland, perhaps resulting in a constant winter flux of more concentrated, basally-derived DOC. The likelihood and broader implications of this export depend on whether the labile fractions of glacial organic carbon survive biogeochemical processing in the proglacial and estuarine regions. Further study is needed in order to determine if the labile fraction has a radiocarbon depleted signature. If it does, more study is also required to fully determine the mechanisms which cause glacial organic carbon to be paradoxically radiocarbon depleted, yet also still retain some labile components. Here we propose two broad mechanisms to explain glacially-derived organic carbon that is both labile and radiocarbon depleted: (1) *in situ* microbial activity utilizing radiocarbon depleted subglacial or supraglacial organic carbon stores, and thereby producing ^{14}C-depleted proteinaceous material, or (2) labile components of the original overridden organic matter remain that have been preserved under the ice sheet. Conceivably, both of these processes could be occurring simultaneously, with regions populated by subglacial microbial communities accessed by the distributed drainage system during low flow periods, and isolated organic carbon stores tapped by headward progression of the subglacial drainage system at the peak summer meltseason.

ACKNOWLEDGMENTS

This research was supported by: the WHOI Clark Arctic Research Initiative (E.B.K., S.B.D., M.A.C.), the National Science and Engineering Research Council of Canada (M.P.B.), the WHOI Ocean and Climate Change Institute (M.P.B.), and a Horton Hydrology Grant from the American Geophysical Union (M.P.B.). We are grateful to P. Henderson for conducting the POC and nutrient analyses, to M. Lafreniere and S. Koziar for assistance with the ion chromatography analyses, to M. Nieto-Cid and J. Becker for assistance with the DOC analyses, to A. McNichol and the NOSAMS prep lab staff for assistance with the radiocarbon analyses, to A. Pearson, M. Tranter and D. Griffith for helpful conversations, to K. Longnecker for comments that improved the manuscript, to M. Behn, I. Joughin, and K. Poinar for assistance in sampling the inland ice, and to B. Gready, P. Henderson, A. Criscitiello, and M. Evans for their valuable assistance in the field. Finally, we thank three anonymous reviewers and the associate editor for comments that greatly improved the manuscript.

APPENDIX A. SUPPLEMENTARY DATA

Supplementary data associated with this article can be found, in the online version, at http://dx.doi.org/10.1016/j.gca.2013.02.006.

REFERENCES

Alley R. B., Andrews J. T., Brigham-Grette J., Clarke G. K. C., Cuffey K. M., Fitzpatrick J. J., Funder S., Marshall S. J., Miller G. H., Mitrovica J. X., Muhs D. R., Otto-Bliesner B. L., Polyak L. and White J. W. C. (2010) History of the Greenland Ice Sheet: paleoclimatic insights. *Quat. Sci. Rev.* **29**, 1728–1756.

Bamber J., van den Broeke M., Ettema J., Lenaerts J. and Rignot E. (2012) Recent large increases in freshwater fluxes from Greenland into the North Atlantic. *Geophys. Res. Lett.* **39**, L19501.

Barker J. D., Sharp M. J., Fitzsimons S. J. and Turner R. J. (2006) Abundance and dynamics of dissolved organic carbon in glacier systems. *Arct. Antarct. Alp. Res.* **38**, 163–172.

Bartholomew I., Nienow P., Mair D., Hubbard A., King M. A. and Sole A. (2010) Seasonal evolution of subglacial drainage and acceleration in a Greenland outlet glacier. *Nat. Geosci.* **3**, 408–411.

Beaupre S. R., Druffel E. R. M. and Griffin S. (2007) A low-blank photochemical extraction system for concentration and isotopic analyses of marine dissolved organic carbon. *Limnol. Oceanogr. Methods* **5**, 174–184.

Benner R., Benitez-Nelson B., Kaiser K. and Amon R. M. W. (2004) Export of young terrigenous dissolved organic carbon from rivers to the Arctic Ocean. *Geophys. Res. Lett.* **31**.

Bhatia M., Das S. B., Kujawinski E. B., Henderson P., Burke A. and Charette M. A. (2011) Seasonal evolution of water contributions to discharge from a Greenland outlet glacier: insight from a new isotope-mixing model. *J. Glaciol.* **57**, 929–941.

Bhatia M., Das S. B., Longnecker K., Charette M. A. and Kujawinski E. B. (2010) Molecular characterization of dissolved organic matter associated with the Greenland ice sheet. *Geochim. Cosmochim. Acta* **74**, 3768–3784.

Bhatia M., Sharp M. and Foght J. (2006) Distinct bacterial communities exist beneath a high arctic polythermal glacier. *Appl. Environ. Microbiol.* **72**, 5838–5845.

Brink N. W. T. and Weidick A. (1974) Greenland ice sheet history since the last glaciation. *Quat. Res.* **4**, 429–440.

Carpenter E. J., Lin S. J. and Capone D. G. (2000) Bacterial activity in South Pole snow. *Appl. Environ. Microbiol.* **66**, 4514–4517.

Cheng S. M. and Foght J. M. (2007) Cultivation-independent and -dependent characterization of Bacteria resident beneath John Evans Glacier. *FEMS Microbiol. Ecol.* **59**, 318–330.

Cooper L. (1988) Isotopic fractionation in snow cover. In *Isotope Tracers in Catchment Hydrology* (eds. C. Kendall and J. McDonnell). Elsevier Science B.V, Amsterdam, pp. 119–136.

Das S. B., Joughin I., Behn M. D., Howat I. M., King M. A., Lizarralde D. and Bhatia M. P. (2008) Fracture propagation to the base of the Greenland Ice Sheet during supraglacial lake drainage. *Science* **320**, 778–781.

Dittmar T. and Kattner G. (2003) The biogeochemistry of the river and shelf ecosystem of the Arctic Ocean: a review. *Mar. Chem.* **83**, 103–120.

Druffel E. R. M. and Bauer J. E. (2000) Radiocarbon distributions in Southern Ocean dissolved and particulate organic matter. *Geophys. Res. Lett.* **27**, 1495–1498.

Dubnick A., Barker J., Sharp M., Wadham J., Lis G., Telling J., Fitzsimons S. and Jackson M. (2010) Characterization of dissolved organic matter (DOM) from glacial environments using total fluorescence spectroscopy and parallel factor analysis. *Ann. Glaciol.* **51**, 111–122.

Escher A. (1971) *Map Sheet no. 3 Sondre Stromfjord – Nugssu aq Geological Maps of Greenland 1:500,000*. Geological Survey of Denmark and Greenland (GEUS), Copenhagen.

Hedges J. I., Keil R. G. and Benner R. (1997) What happens to terrestrial organic matter in the ocean? *Org. Geochem.* **27**, 195–212.

Hodson A., Anesio A. M., Tranter M., Fountain A., Osborn M., Priscu J., Laybourn-Parry J. and Sattler B. (2008) Glacial ecosystems. *Ecol. Monogr.* **78**, 41–67.

Hodson A., Boggild C., Hanna E., Huybrechts P., Langford H., Cameron K. and Houldsworth A. (2010) The cryoconite ecosystem on the Greenland ice sheet. *Ann. Glaciol.* **51**, 123–129.

Hood E., Fellman J., Spencer R. G. M., Hernes P. J., Edwards R., D'Amore D. and Scott D. (2009) Glaciers as a source of ancient and labile organic matter to the marine environment. *Nature* **462**, 1044–U1100.

Hood E. and Scott D. (2008) Riverine organic matter and nutrients in southeast Alaska affected by glacial coverage. *Nat. Geosci.* **1**, 583–587.

Kujawinski E. B., Longnecker K., Blough N. V., Vecchio R. D., Finlay L., Kitner J. B. and Giovannoni S. J. (2009) Identification of possible source markers in marine dissolved organic matter using ultrahigh resolution mass spectrometry. *Geochim. Cosmochim. Acta* **73**, 4384–4399.

Lafreniere M. and Lamoureux S. (2008) Seasonal dynamics of dissolved nitrogen exports from two High Arctic watersheds, Melville Island, Canada. *Hydrol. Res.* **39**, 323–335.

Lafreniere M. J. and Sharp M. J. (2004) The concentration and fluorescence of dissolved organic carbon (DOC) in glacial and nonglacial catchments: interpreting hydrological flow routing and DOC sources. *Arct. Antarct. Alp. Res.* **36**, 156–165.

Mayorga E., Aufdenkampe A. K., Masiello C. A., Krusche A. V., Hedges J. I., Quay P. D., Richey J. E. and Brown T. A. (2005) Young organic matter as a source of carbon dioxide outgassing from Amazonian rivers. *Nature* **436**, 538–541.

McNichol A. P. and Aluwihare L. I. (2007) The power of radiocarbon in biogeochemical studies of the marine carbon cycle: Insights from studies of dissolved and particulate organic carbon (DOC and POC). *Chem. Rev.* **107**, 443–466.

Millot R., Gaillardet J., Dupre B. and Allegre C. J. (2003) Northern latitude chemical weathering rates: clues from the Mackenzie River Basin, Canada. *Geochim. Cosmochim. Acta* **67**, 1305–1329.

Pautler B. G., Simpson A. J., Simpson M. J., Tseng L.-H., Spraul M., Dubnick A., Sharp M. J. and Fitzsimons S. J. (2011) Detection and structural identification of dissolved organic matter in Antarctic Glacial Ice at Natural Abundance by SPR-W5-WATERGATE (1)H NMR spectroscopy. *Environ. Sci. Technol.* **45**, 4710–4717.

Pautler B. G., Woods G. C., Dubnick A., Simpson A. J., Sharp M. J., Fitzsimons S. J. and Simpson M. J. (2012) Molecular characterization of dissolved organic matter in glacial ice: coupling natural abundance ^{1}H NMR and fluorescence spectroscopy. *Environ. Sci. Technol.*.

Petsch S. T., Eglinton T. I. and Edwards K. J. (2001) C-14-dead living biomass: evidence for microbial assimilation of ancient organic carbon during share weathering. *Science* **292**, 1127–1131.

Raymond P. A. and Bauer J. E. (2001a) Riverine export of aged terrestrial organic matter to the North Atlantic Ocean. *Nature* **409**, 497–500.

Raymond P. A. and Bauer J. E. (2001b) Use of ^{14}C and ^{13}C natural abundances for evaluating riverine, estuarine, and coastal DOC and POC sources and cycling: a review and synthesis. *Org. Geochem.* **32**, 469–485.

Raymond P. A., McClelland J. W., Holmes R. M., Zhulidov A. V., Mull K., Peterson B. J., Striegl R. G., Aiken G. R. and Gurtovaya T. Y. (2007) Flux and age of dissolved organic carbon exported to the Arctic Ocean: a carbon isotopic study of the five largest arctic rivers. *Global Biogeochem. Cycles* **21**.

Schneider R. J., Jones G. A., McNichol A. P., Vonreden K. F., Elder K. L., Huang K. and Kessel E. D. (1994) Methods for data screening, flagging and error analysis at the national ocean sciences AMS facility. *Nucl. Instrum. Methods Phys. Res. Sect. B: Beam Interactions with Materials and Atoms* **92**, 172–175.

Sharp M., Parkes J., Cragg B., Fairchild I. J., Lamb H. and Tranter M. (1999) Widespread bacterial populations at glacier beds and their relationship to rock weathering and carbon cycling. *Geology* **27**, 107–110.

Singer G. A., Fasching C., Wilhelm L., Niggemann J., Steier P., Dittmar T. and Battin T. J. (2012) Biogeochemically diverse organic matter in Alpine glaciers and its downstream fate. *Nat. Geosci.* **5**, 710–714.

Skidmore M., Anderson S. P., Sharp M., Foght J. and Lanoil B. D. (2005) Comparison of microbial community compositions of two subglacial environments reveals a possible role for microbes in chemical weathering processes. *Appl. Environ. Microbiol.* **71**, 6986–6997.

Skidmore M., Tranter M., Tulaczyk S. and Lanoil B. (2010) Hydrochemistry of ice stream beds – evaporitic or microbial effects? *Hydrol. Processes* **24**, 517–523.

Skidmore M. L., Foght J. M. and Sharp M. J. (2000) Microbial life beneath a high Arctic glacier. *Appl. Environ. Microbiol.* **66**, 3214–3220.

Stibal M., Telling J., Cook J., Mak K. M., Hodson A. and Anesio A. M. (2012) Environmental controls on microbial abundance and activity on the Greenland Ice Sheet: a multivariate analysis approach. *Microb. Ecol.* **63**, 74–84.

Stibal M., Tranter M., Benning L. G. and Rehak J. (2008) Microbial primary production on an Arctic glacier is insignificant in comparison with allochthonous organic carbon input. *Environ. Microbiol.* **10**, 2172–2178.

Stubbins A., Hood E., Raymond P. A., Aiken G. R., Sleighter R. L., Hernes P. J., Butman D., Hatcher P. G., Striegl R. G., Schuster P., Abdulla H. A. N., Vermilyea A. W., Scott D. T.

and Spencer R. G. M. () Anthropogenic aerosols as a source of ancient dissolved organic matter in glaciers. *Nat. Geosci.* **5**, 198–201.

Stuiver M. and Polach H. A. (1977) Reporting of C-14 data – discussion. *Radiocarbon* **19**, 355–363.

Tranter M. (2003) Geochemical Weathering in Glacial and Proglacial Environments. In (eds. J. I. Drever). Elsevier. pp. 189–205.

Tranter M., Sharp M. J., Lamb H. R., Brown G. H., Hubbard B. P. and Willis I. C. (2002) Geochemical weathering at the bed of Haut Glacier d'Arolla, Switzerland – a new model. *Hydrol. Processes* **16**, 959–993.

Tung H. C., Price P. B., Bramall N. E. and Vrdoljak G. (2006) Microorganisms metabolizing on clay grains in 3-km-deep Greenland basal ice. *Astrobiology* **6**, 69–86.

Verardo D. J., Froelich P. N. and McIntyre A. (1990) Determination of organic carbon and nitrogen in marine sediments using the Carlo Erba NA-1500 analyzer. *Deep-Sea Res. Part a – Oceanogr. Res. Papers* **37**, 157–165.

Wadham J. L., Tranter M., Hodson A. J., Hodgkins R., Bottrell S., Cooper R. and Raiswell R. (2010a) Hydro-biogeochemical coupling beneath a large polythermal Arctic glacier: implications for subice sheet biogeochemistry. *J. Geophys. Res. Earth Surf.* **115**.

Wadham J. L., Tranter M., Skidmore M., Hodson A. J., Priscu J., Lyons W. B., Sharp M., Wynn P. and Jackson M. (2010b) Biogeochemical weathering under ice: Size matters. *Global Biogeochem. Cycles* **24**.

Wadham J. L., Tranter M., Tulaczyk S. and Sharp M. (2008) Subglacial methanogenesis: A potential climatic amplifier? *Global Biogeochem. Cycles* **22**.

Weidick A. and Bennike O. (2007) Quaternary glaciation history and glaciology of Jakobshavn Isbrae and the Disko Bugt region, West Greenland: A review. In *Geological Survey of Denmark and Greenland* (ed. M.o.C.a.E.).

Yde J. C., Finster K. W., Raiswell R., Steffensen J. P., Heinemeier J., Olsen J., Gunnlaugsson H. P. and Nielsen O. B. (2010) Basal ice microbiology at the margin of the Greenland ice sheet. *Ann. Glaciol.* **51**, 71–79.

Associate editor: Silke Severmann